

# NATIONAL ADVISORY COMMITTEE FOR AERONAUTICS

TECHNICAL NOTE 3468

EFFECTS OF SWEEP ON THE MAXIMUM-LIFT CHARACTERISTICS  
OF FOUR ASPECT-RATIO-4 WINGS AT TRANSONIC SPEEDS

By Thomas R. Turner

Langley Aeronautical Laboratory  
Langley Field, Va.

**LIBRARY COPY**

JUL 25 1955

LANGLEY AERONAUTICAL LABORATORY  
LIBRARY, NACA  
LANGLEY FIELD, VIRGINIA



Washington

July 1955

## NATIONAL ADVISORY COMMITTEE FOR AERONAUTICS

## TECHNICAL NOTE 3468

## EFFECTS OF SWEEP ON THE MAXIMUM-LIFT CHARACTERISTICS

OF FOUR ASPECT-RATIO-4 WINGS AT TRANSONIC SPEEDS<sup>1</sup>

By Thomas R. Turner

## SUMMARY

An investigation at transonic speeds has been made in the Langley high-speed 7- by 10-foot tunnel to determine the effect of wing sweep on the maximum-lift characteristics of a series of wings having aspect ratio of 4, taper ratio of 0.6, and NACA 65A006 airfoil sections. The Mach number varied from 0.61 to 1.20 with the Reynolds number varying from 380,000 to 460,000.

Maximum lift coefficients increased with increased sweep at the lower Mach numbers but decreased with increased sweep at the higher Mach numbers so that there was less variation of the maximum lift coefficient with Mach number as the sweep was increased.

## INTRODUCTION

A knowledge of the effects of sweep and Mach number on wing aerodynamic characteristics near maximum lift is becoming of greater importance as the speeds and altitudes flown by modern aircraft continue to increase. High-speed, high-altitude aircraft fly at rather high lift coefficients and may reach or exceed the angle of attack for the maximum lift of the aircraft in maneuvers. Since sweptback wings are being used to delay and to minimize the effects of compressibility on some aircraft, it is important that the effects of sweep on the maximum lift coefficient be known.

There are considerable data available for both swept and unswept wings up to maximum lift at low Mach numbers (for example, reference 1), but only a limited amount is available above a Mach number of approximately 0.60.

This paper presents the results obtained from an investigation to determine the effects of sweep on the maximum-lift characteristics of a

---

<sup>1</sup>Supersedes recently declassified NACA RM L50H11, 1950.

series of aspect-ratio-4 wings with the quarter-chord line swept back  $0^\circ$ ,  $35^\circ$ ,  $45^\circ$ , and  $60^\circ$  through the Mach number range from 0.61 to 1.20.

# COEFFICIENTS AND SYMBOLS

$C_L$	lift coefficient, $L/qS$
$C_D$	drag coefficient, $D/qS$
$C_m$	pitching-moment coefficient, $M'/qS\bar{c}$
$L$	twice measured lift of semispan wing, lb
$D$	twice measured drag of semispan wing, lb
$M'$	twice measured pitching moment of semispan wing about $0.25\bar{c}$ , ft-lb
$C_{L_{max}}$	maximum lift coefficient
$L/D$	lift-drag ratio
$R$	Reynolds number
$M$	Mach number, $V/a$
$M_l$	local Mach number
$V$	stream velocity, ft/sec
$a$	velocity of sound, ft/sec
$q$	dynamic pressure, $\frac{1}{2}\rho V^2$ , lb/sq ft
$\rho$	mass density of air, slugs/cu ft
$\alpha$	angle of attack, deg
$S$	twice area of semispan wing, sq ft
$\bar{c}$	wing mean aerodynamic chord, measured parallel to plane of symmetry, $\frac{2}{S} \int_0^{b/2} c^2 dy$ , ft
$b$	twice-span of reflection-plane wing, ft

c	local wing chord parallel to plane of symmetry, ft
$c_r$	wing root chord, ft
$c_t$	wing tip chord, ft
y	spanwise distance from plane of symmetry, ft
$\Lambda$	sweepback of quarter-chord line, deg

#### MODELS AND TEST TECHNIQUE

The four semispan models used in this investigation had NACA 65A006 sections parallel to the plane of symmetry, an aspect ratio of 4 (based on complete wing), a taper ratio of 0.60, and the quarter-chord line swept back  $0^\circ$ ,  $35^\circ$ ,  $45^\circ$ , and  $60^\circ$  (fig. 1). The  $0^\circ$ ,  $35^\circ$ , and  $60^\circ$  swept-back models were made of steel and the  $45^\circ$  sweptback model was made of beryllium copper. A circular end plate 2.625 inches in diameter was fastened to the root section of each wing to cover a 2.187-inch-diameter hole cut in the bump surface to clear the wing butt (fig. 2).

The investigation was made in the high-velocity field of flow over the Langley high-speed 7- by 10-foot-tunnel transonic bump. Some details of the bump and bump-testing technique are given in reference 2. A sketch showing the relative size of the model and bump is shown in figure 3. The velocity distribution in the vicinity of the model is shown in figure 4. Outlines of the  $\Lambda = 0^\circ$  and  $\Lambda = 60^\circ$  wings have been superimposed on this figure in order to illustrate the extent of the spanwise and chordwise gradients in Mach number. The test Mach number is the average Mach number over the span and chord of the model and is obtained from charts similar to figure 4. The effect of the Mach number gradient over the model has been neglected in the results presented.

The variation of Reynolds number with Mach number for the investigation is presented in figure 5.

The forces and moments on the models were measured by means of an electrical strain-gage balance submerged in the bump and wired to an indicator outside the tunnel.

## RESULTS AND DISCUSSION

Lift characteristics.— The variation of lift coefficient with angle of attack (figs. 6 to 9) shows that extremely large angles of attack are required to obtain maximum lift coefficient when the wing is swept back. The variation of lift coefficient with angle of attack is small at angles of attack near maximum lift coefficient, and, in general, the loss in lift coefficient beyond  $C_{L_{max}}$  is gradual.

Since no corrections for wing flexibility or end-plate interference have been made, the lift-curve slopes taken from these data will have only limited value. In general, however, the lift-curve slope decreases with increasing sweepback at a constant Mach number, as would be expected.

The variation of  $C_{L_{max}}$  with Mach number is presented in figure 10. The  $C_{L_{max}}$  values at a Mach number of 0.10 are from reference 1 at a Reynolds number of approximately 3,000,000 and show a reasonable relation to the high Mach number, low Reynolds number values of the present investigation. The effect of the wing-root end plate has been neglected for this investigation; however, some unpublished experimental results obtained in a previous investigation indicated that the maximum lift coefficients would be slightly decreased by the presence of the end plate. The maximum lift coefficient increased with increased sweep below a Mach number of about 0.80 and decreased with increased sweep above a Mach number of about 0.95 but appeared to be practically independent of angle of sweep around a Mach number of 0.90 (fig. 10).

The maximum lift coefficient at low supersonic speeds was almost twice the low Mach number value for the wing with zero sweep; however, this variation in  $C_{L_{max}}$  with Mach number decreased with increased wing sweep. The variation of  $C_{L_{max}}$  with Mach number for the 35° and 45° swept wings of this investigation is very similar to the  $C_{L_{max}}$  variation for a thicker 42° sweptback wing reported in reference 3.

Drag characteristics.— Drag coefficients for lift coefficients above approximately 0.20 are presented in figures 11 to 14. The drag coefficients for lift coefficients below approximately 0.20 are omitted because of the unknown value of the end-plate drag which may be large compared with the wing drag. It is believed, however, that this end-plate drag will be a small part of the total drag at the higher lift coefficients.

Lift-drag ratios for the wings at a Mach number of 0.92 and a curve of the cotangent of  $\alpha$  are presented in figure 15. Because of the close agreement of the data for the several wings and the curve of

cotangent  $\alpha$ , it appears that for this series of wings the resultant force is normal to the chord plane for all practical purposes above an angle of attack of approximately  $8^\circ$ . This same relationship was found to exist throughout the Mach range investigated.

Pitching-moment characteristics.— The pitching-moment-coefficient data for the various wings are presented in figures 16 to 19. In general, as was to be expected, the stability of the wings increased ( $C_m/C_L$  became more negative) as the Mach number increased, but the stability decreased ( $C_m/C_L$  became more positive) as wing sweep increased. If the large changes in stability with changes in lift coefficient or angle of attack for these low Reynolds number tests persist at flight Reynolds number, it appears that in some cases severe stability problems may be encountered at large angles of attack.

#### CONCLUDING REMARKS

Results from wind-tunnel tests of a series of swept, aspect-ratio-4 wings at transonic Mach numbers have indicated that:

1. Maximum lift coefficients increased with increased sweep at the lower Mach numbers but decreased with increased sweep at the higher Mach numbers so that there was less variation of the maximum lift coefficient with Mach number as the sweep was increased.
2. The resultant force was, for all practical purposes, normal to the chord plane at angles of attack above approximately  $8^\circ$ .
3. If the large changes in stability with changes in angle of attack or lift coefficient for the low Reynolds number investigation persist at flight Reynolds numbers, it appears that in some cases severe stability problems may be encountered at high lift coefficients or high angles of attack.

Langley Aeronautical Laboratory,  
National Advisory Committee for Aeronautics,  
Langley Field, Va., August 11, 1950.

## REFERENCES

1. Cahill, Jones F., and Gottlieb, Stanley M.: Low-Speed Aerodynamic Characteristics of a Series of Swept Wings Having NACA 65A006 Airfoil Sections. NACA RM L5OF16, 1950.
2. Schneider, Leslie E., and Ziff, Howard L.: Preliminary Investigation of Spoiler Lateral Control on a  $42^\circ$  Sweptback Wing at Transonic Speeds. NACA RM L7F19, 1947.
3. Turner, Thomas R.: Maximum-Lift Investigation at Mach Numbers from 0.05 to 1.20 of a Wing with Leading Edge Swept Back  $42^\circ$ . NACA RM L9K03, 1950.

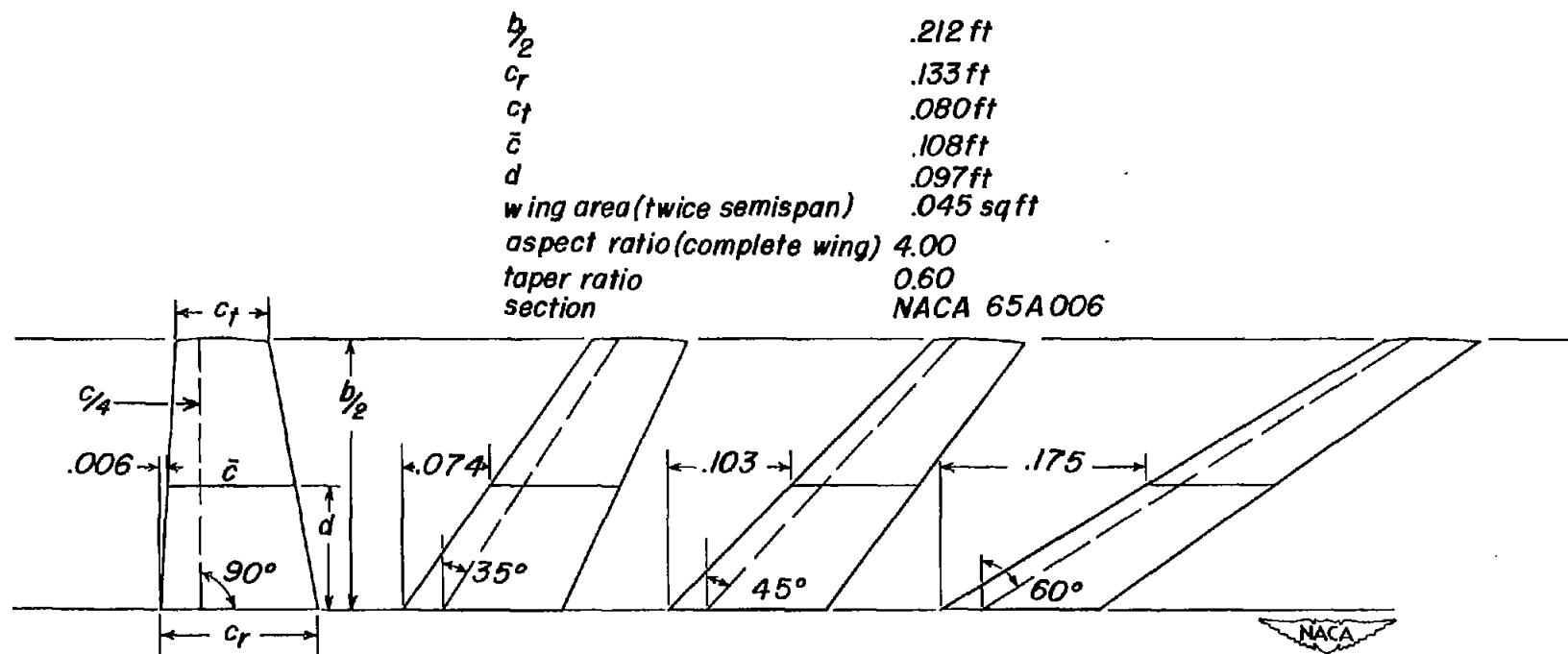


Figure 1.- Geometric characteristics of wings investigated. Dimensions in feet.



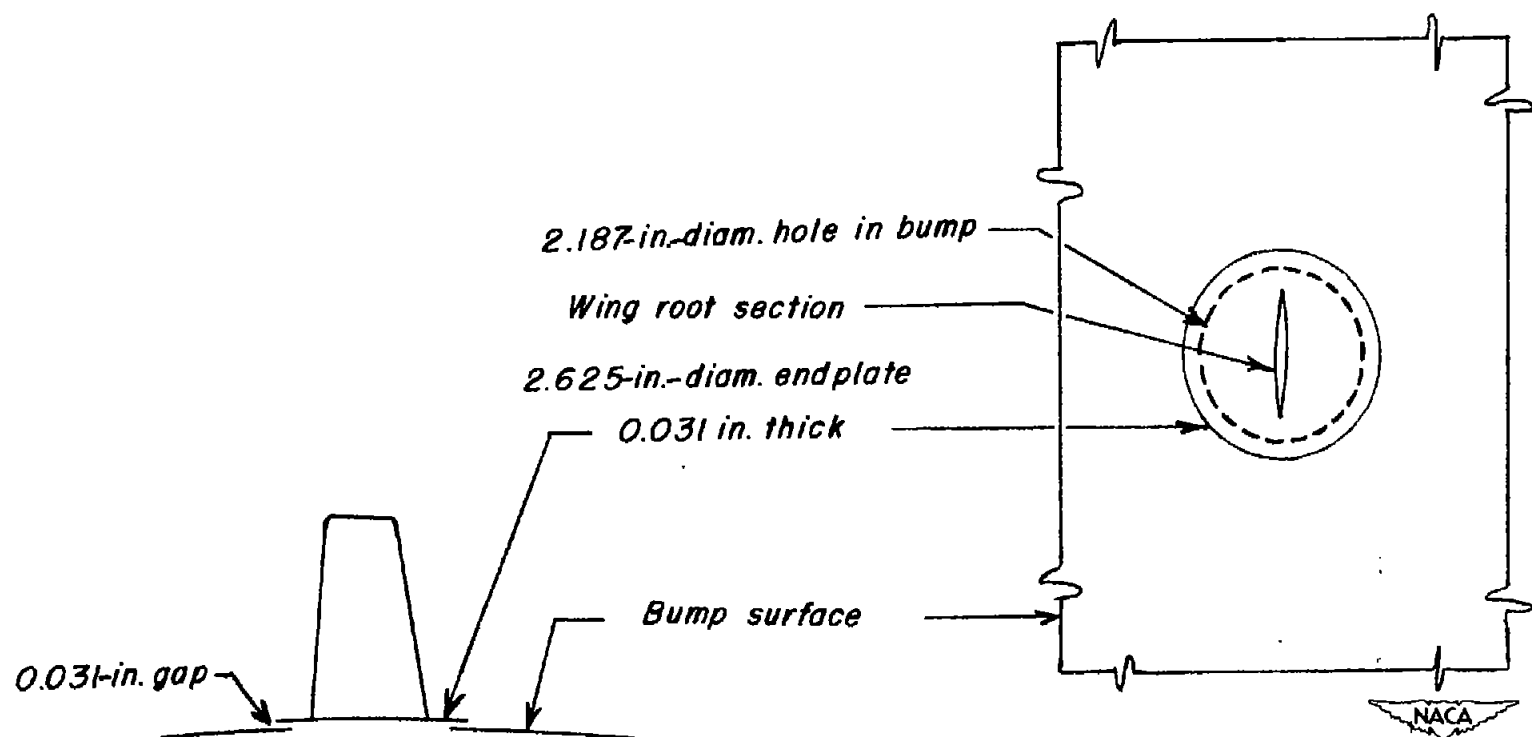


Figure 2.- Details of wing-root end plate and gaps.

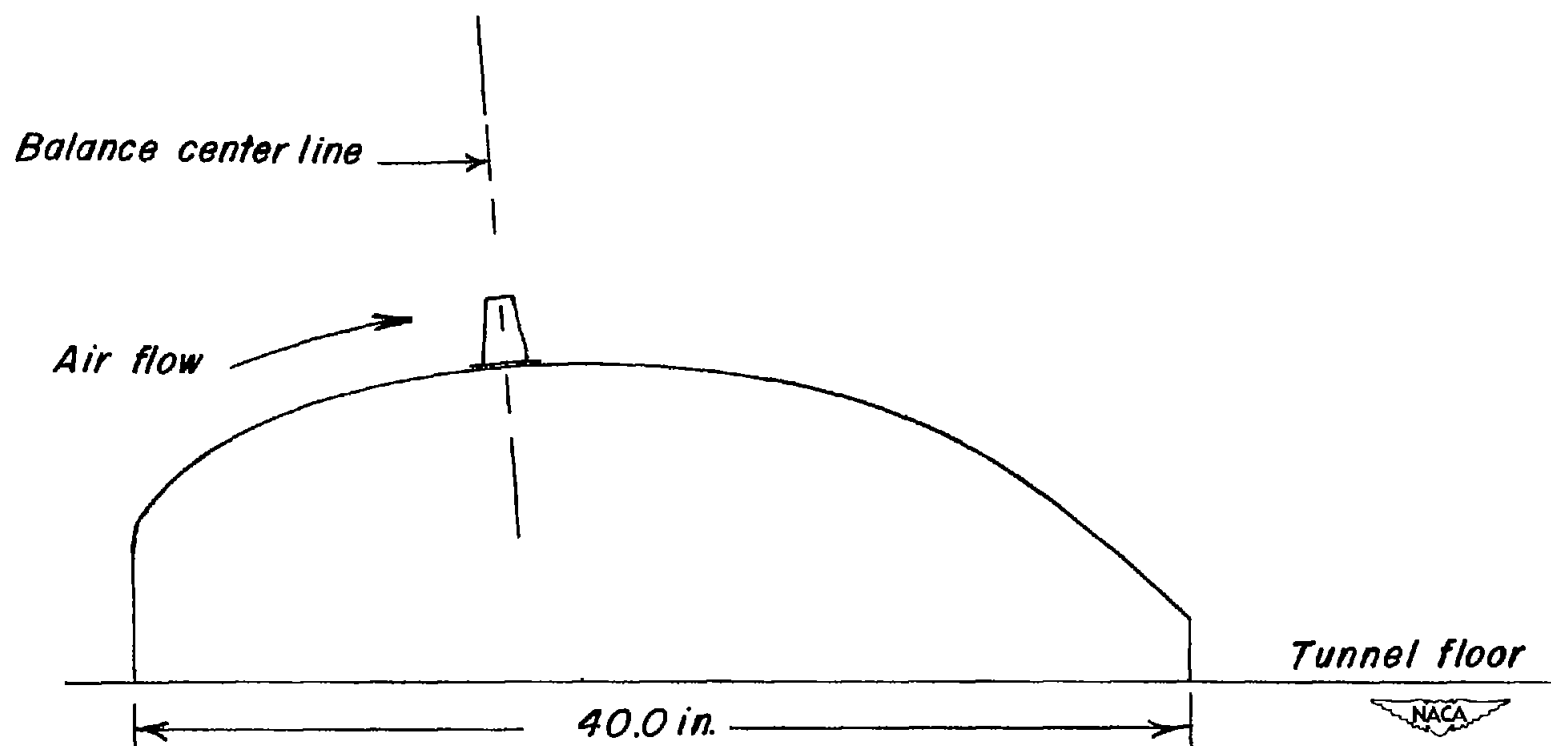


Figure 3.- Schematic sketch of relative position of model, balance, and transonic bump as mounted in the Langley high-speed 7- by 10-foot tunnel.

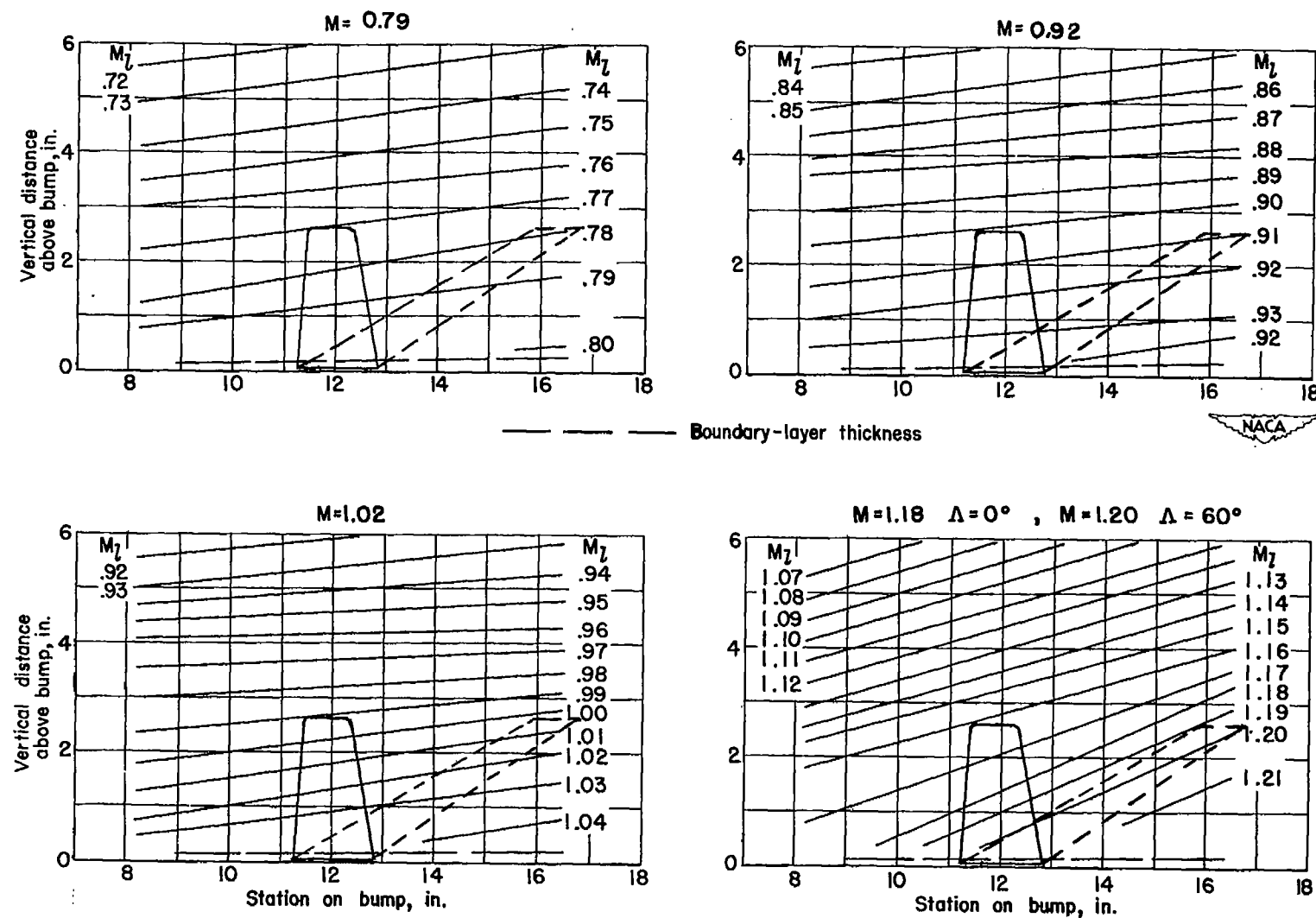


Figure 4.- Typical Mach number contours over transonic bump in region of model location.

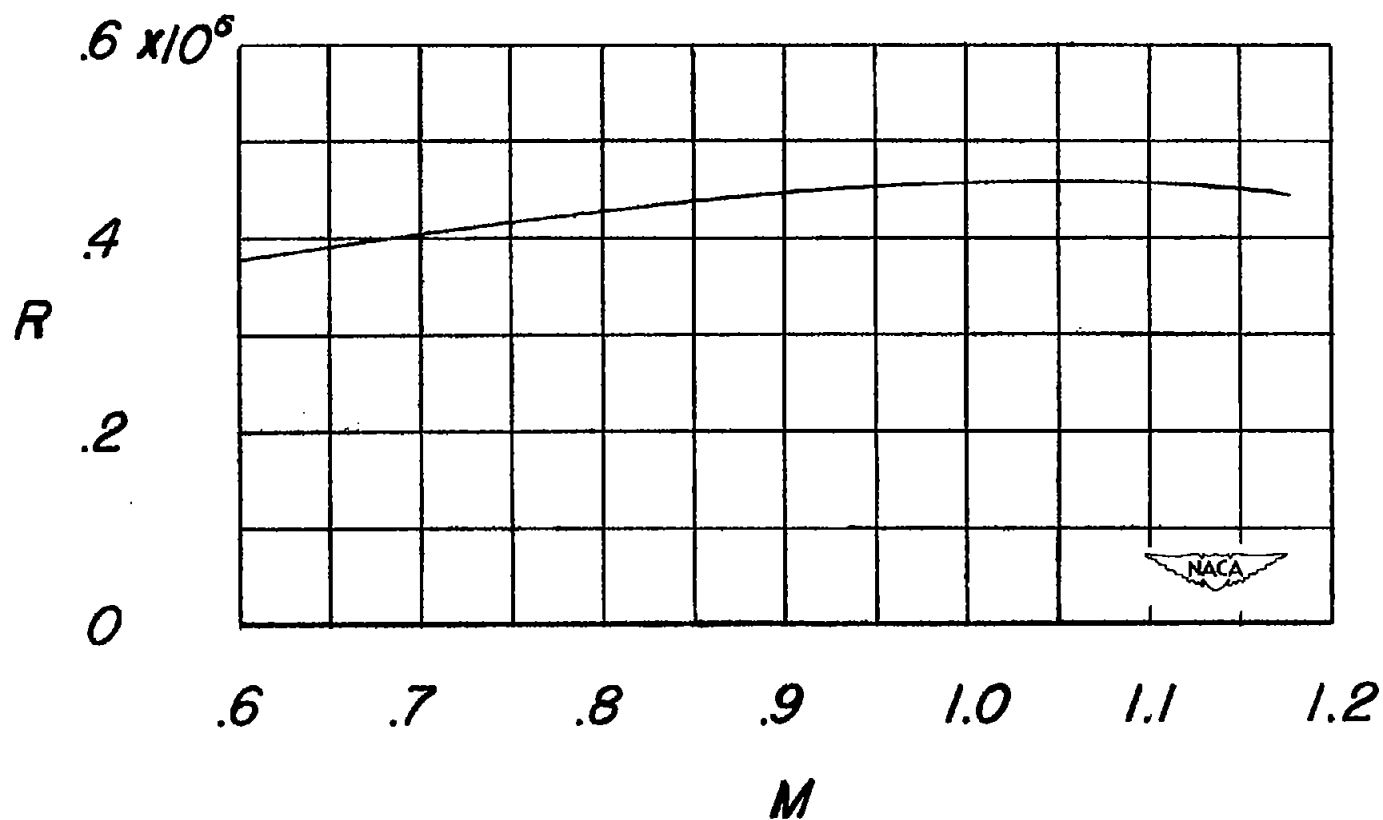


Figure 5.- Variation of Reynolds number with Mach number for the investigation.

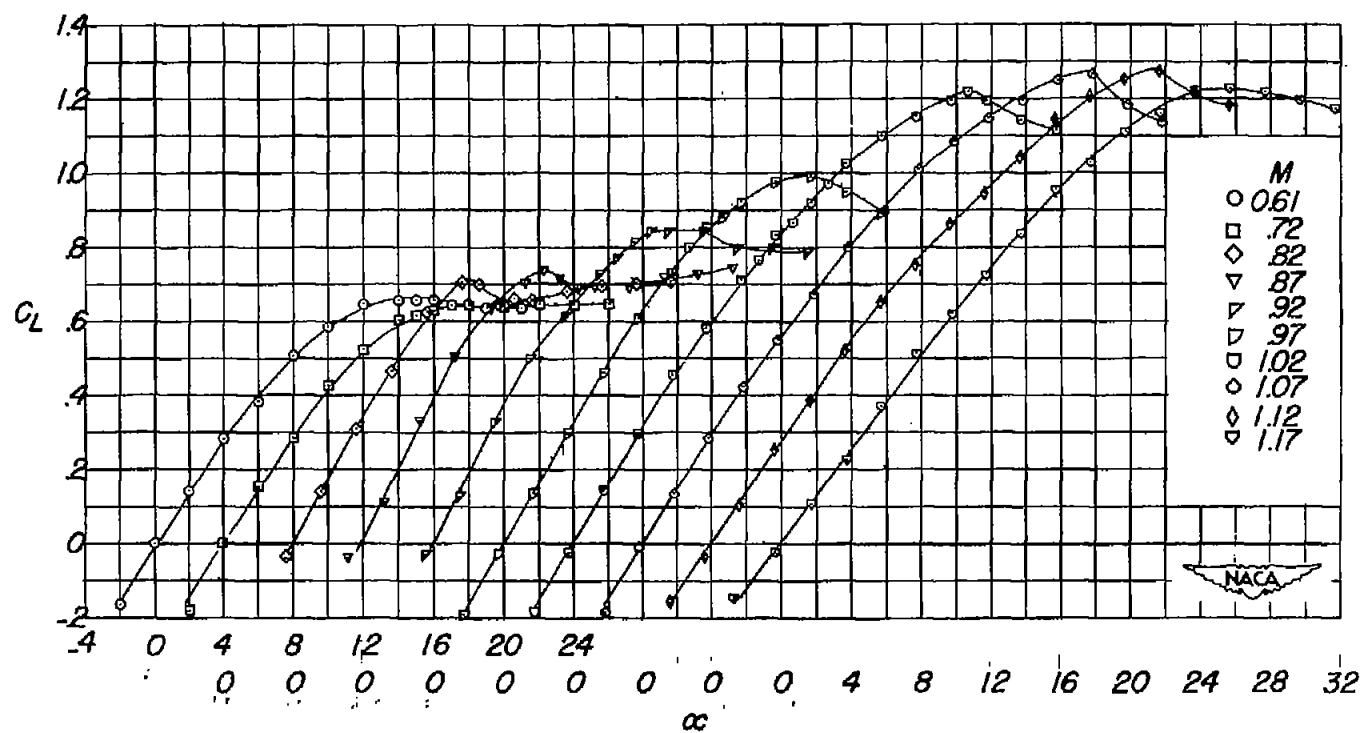


Figure 6.- Variation of lift coefficient with angle of attack for an aspect-ratio-4 wing.  $\Lambda = 0^\circ$ .

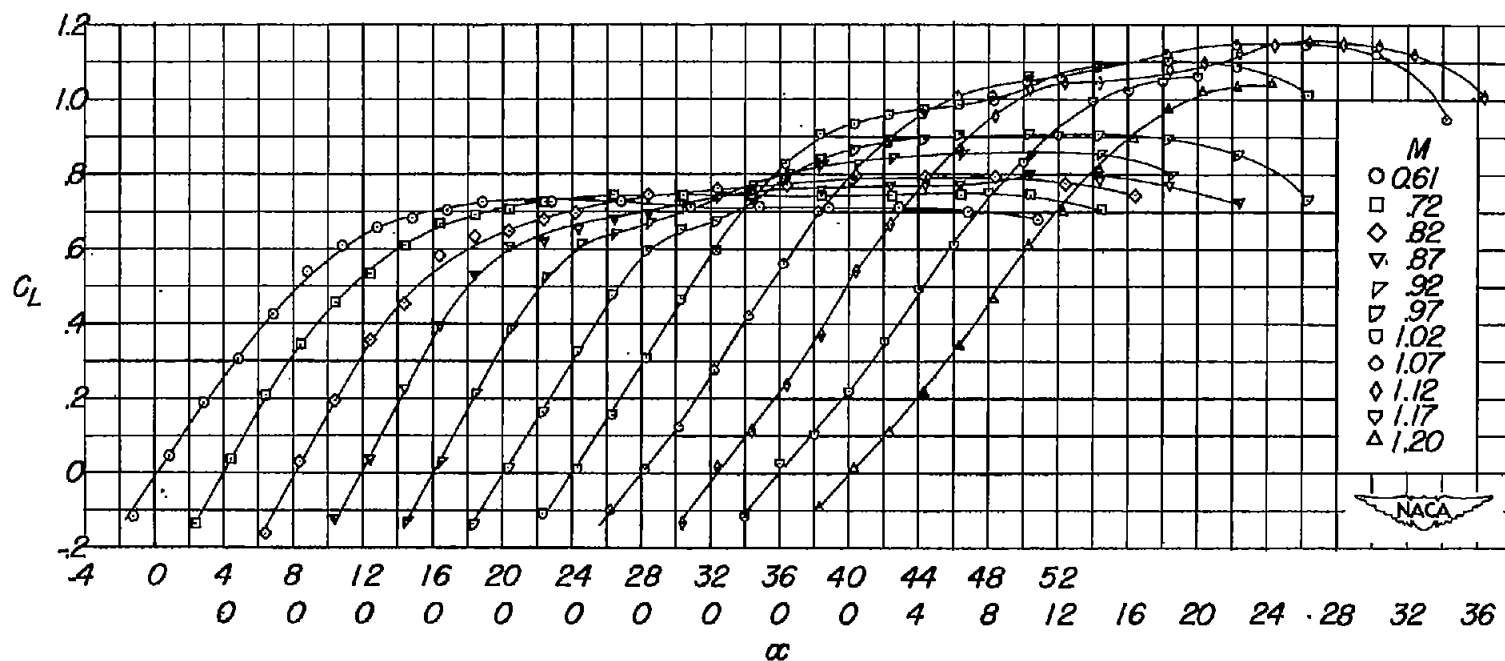


Figure 7.- Variation of lift coefficient with angle of attack for an aspect-ratio-4 wing.  $\Lambda = 35^\circ$ .

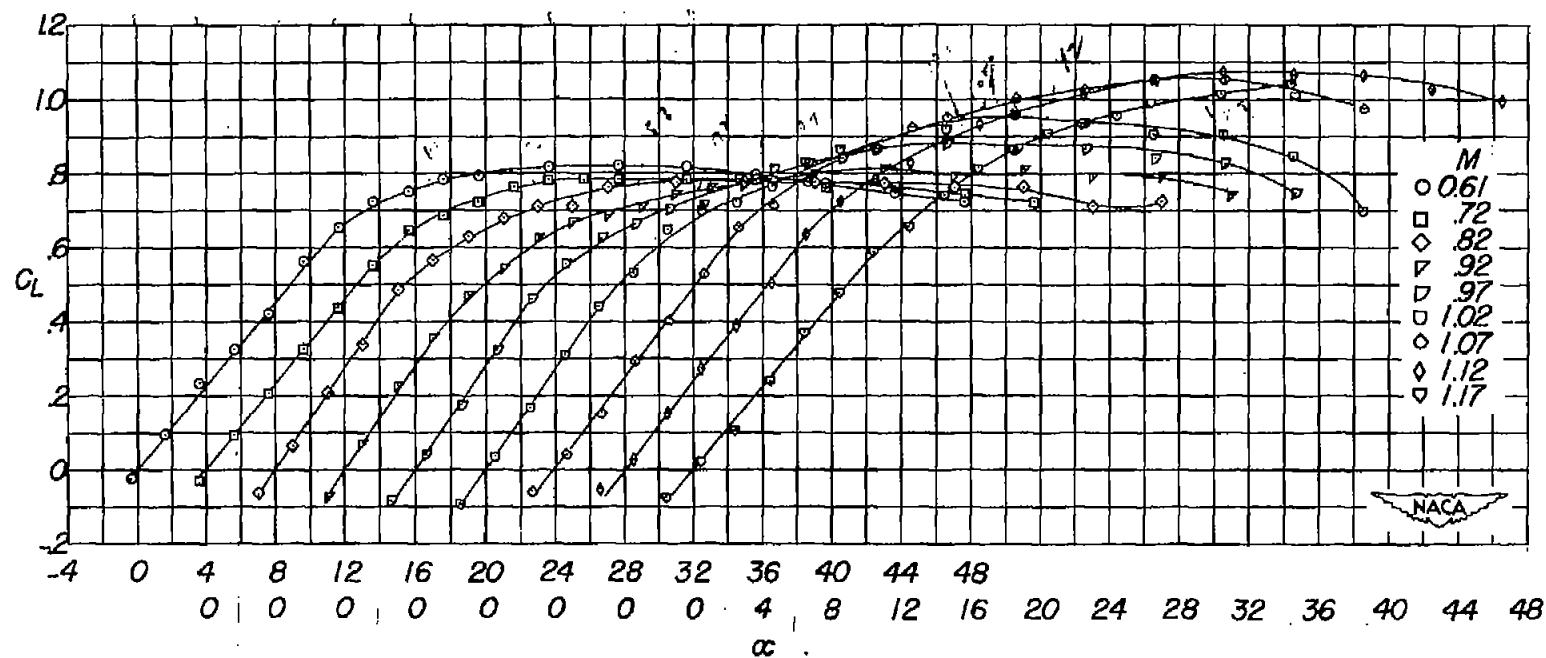


Figure 8.- Variation of lift coefficient with angle of attack for an aspect-ratio-4 wing.  $\Lambda = 45^\circ$ .

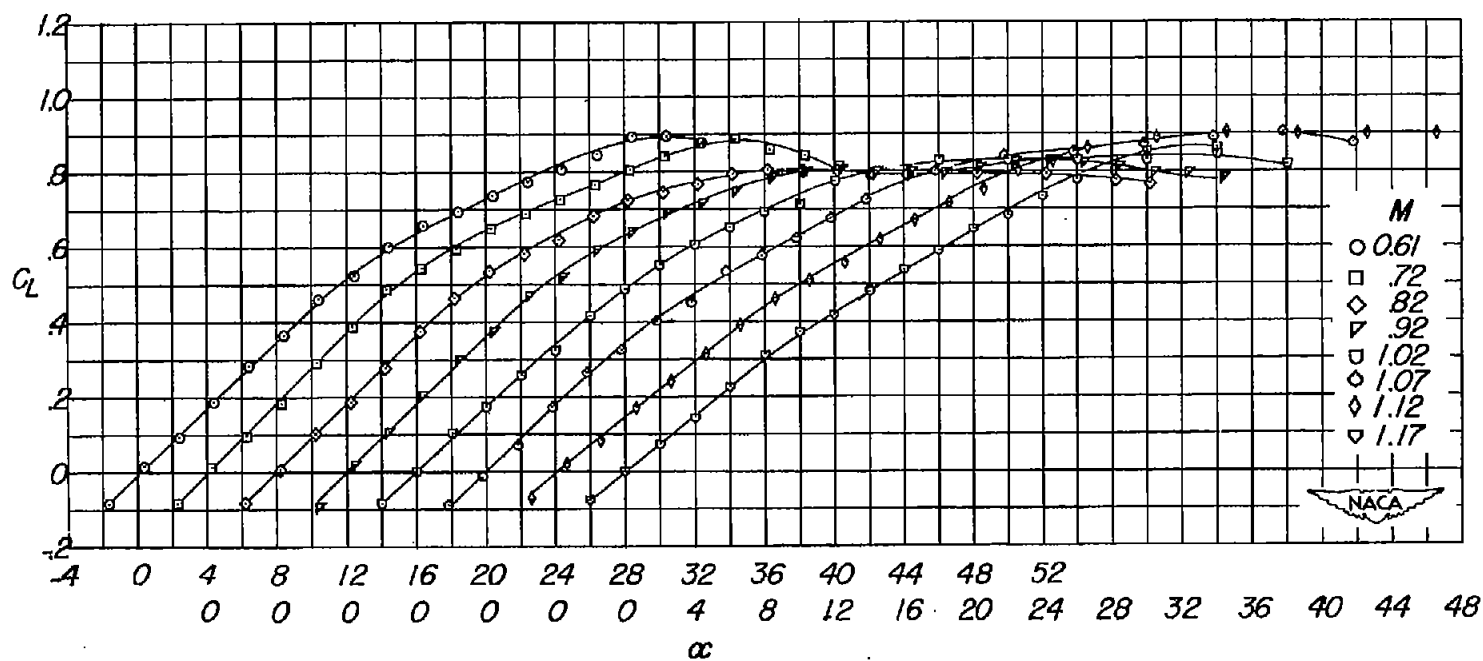


Figure 9.- Variation of lift coefficient with angle of attack for an aspect-ratio-4 wing.  $\Lambda = 60^\circ$ .



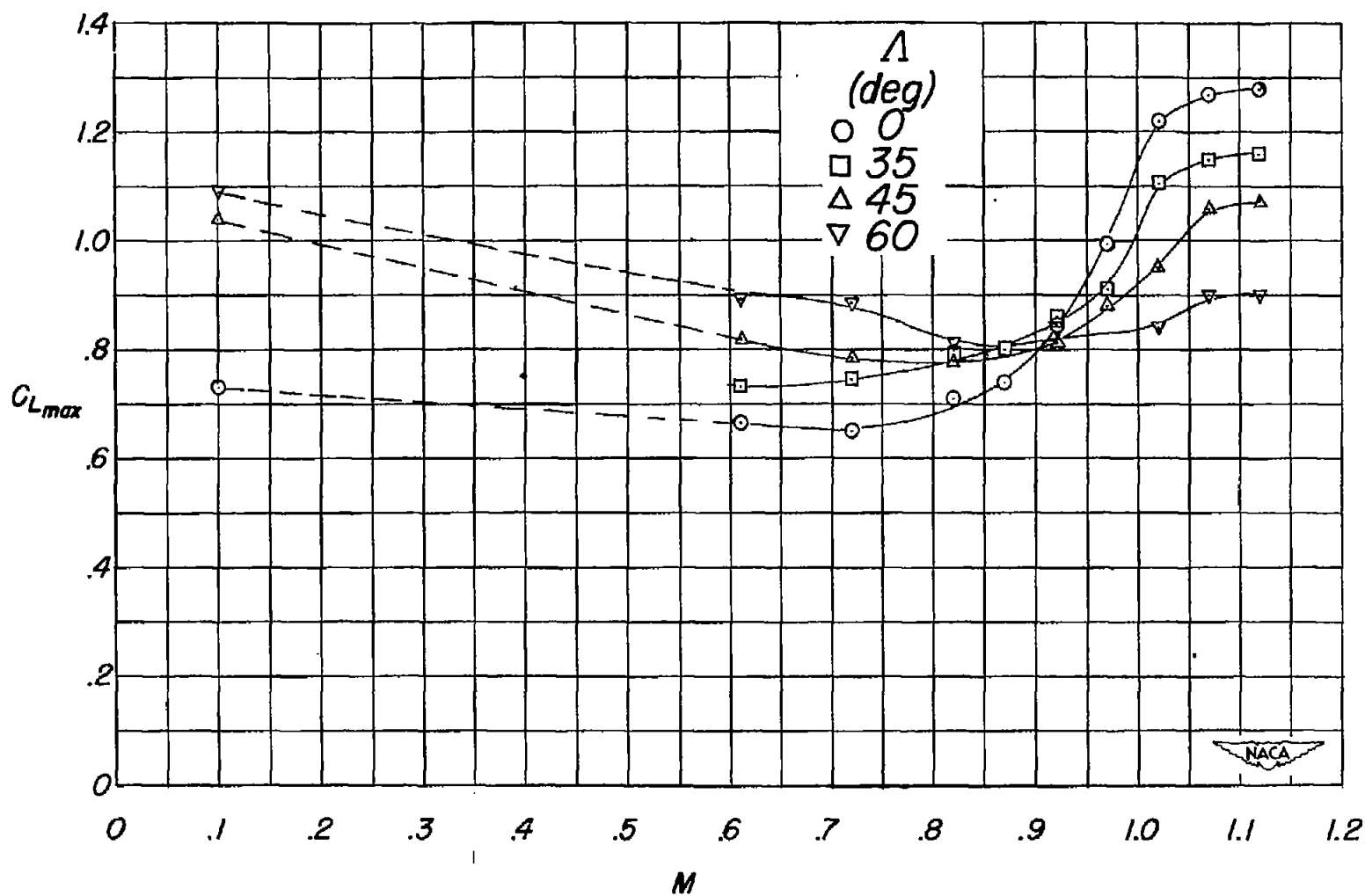


Figure 10.- Effect of sweep on maximum lift coefficient at transonic Mach numbers for an aspect-ratio-4 wing.

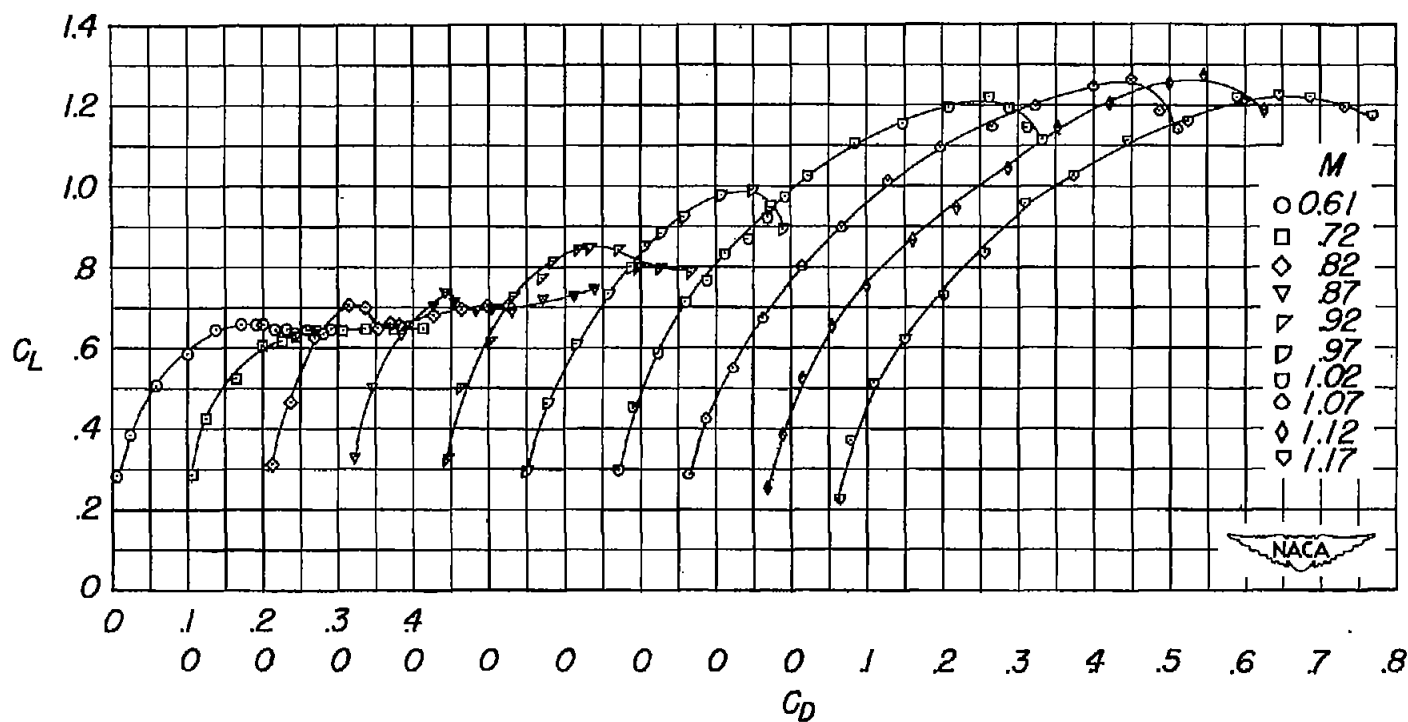


Figure 11.- Variation of drag coefficient with lift coefficient for an aspect-ratio-4 wing.  $\Lambda = 0^\circ$ .

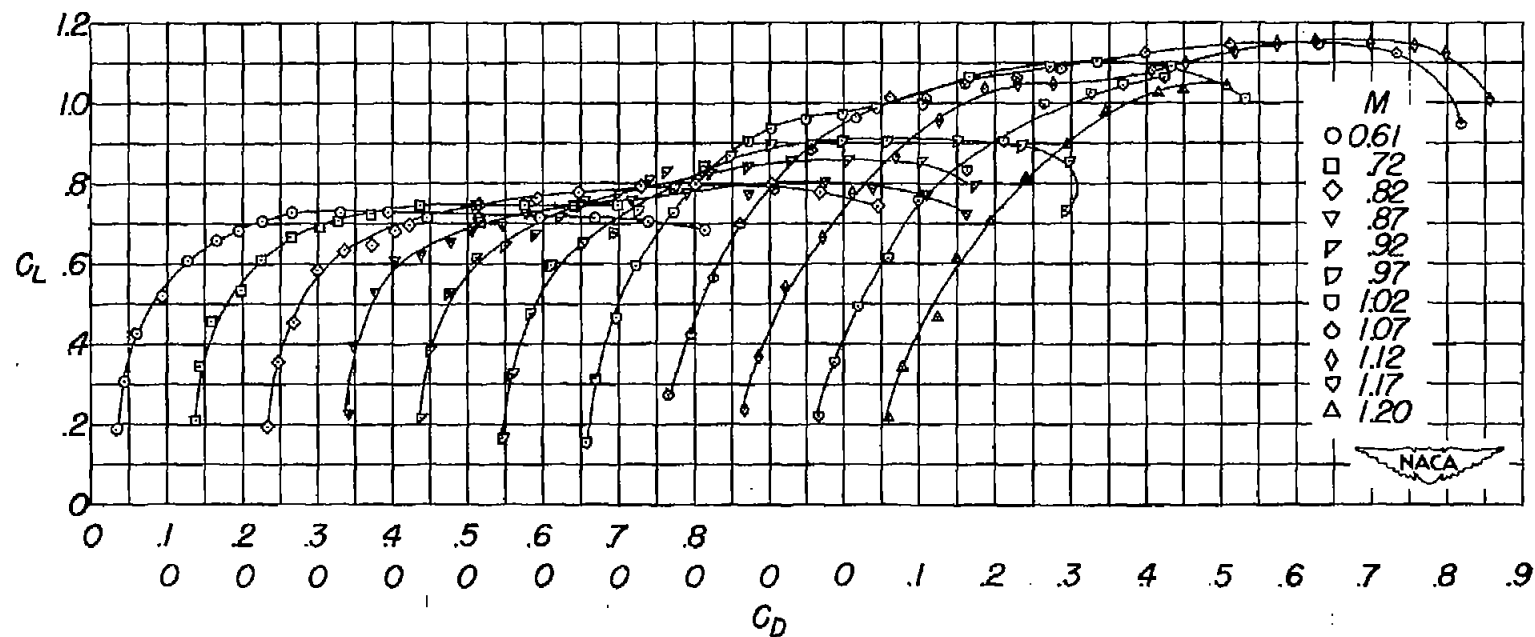


Figure 12.- Variation of drag coefficient with lift coefficient for an aspect-ratio-4 wing.  $\Lambda = 35^\circ$ .

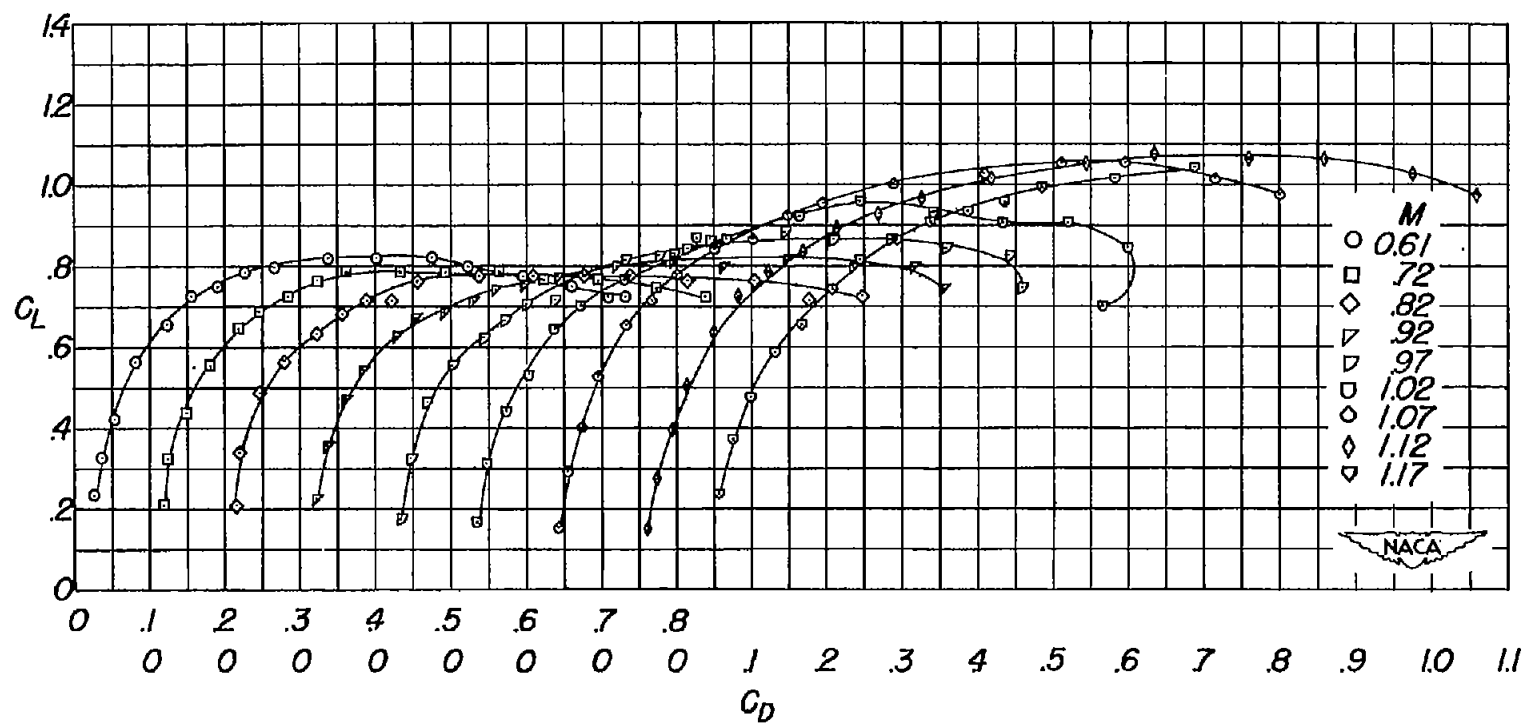


Figure 13.- Variation of drag coefficient with lift coefficient for an aspect-ratio-4 wing.  $\Lambda = 45^\circ$ .

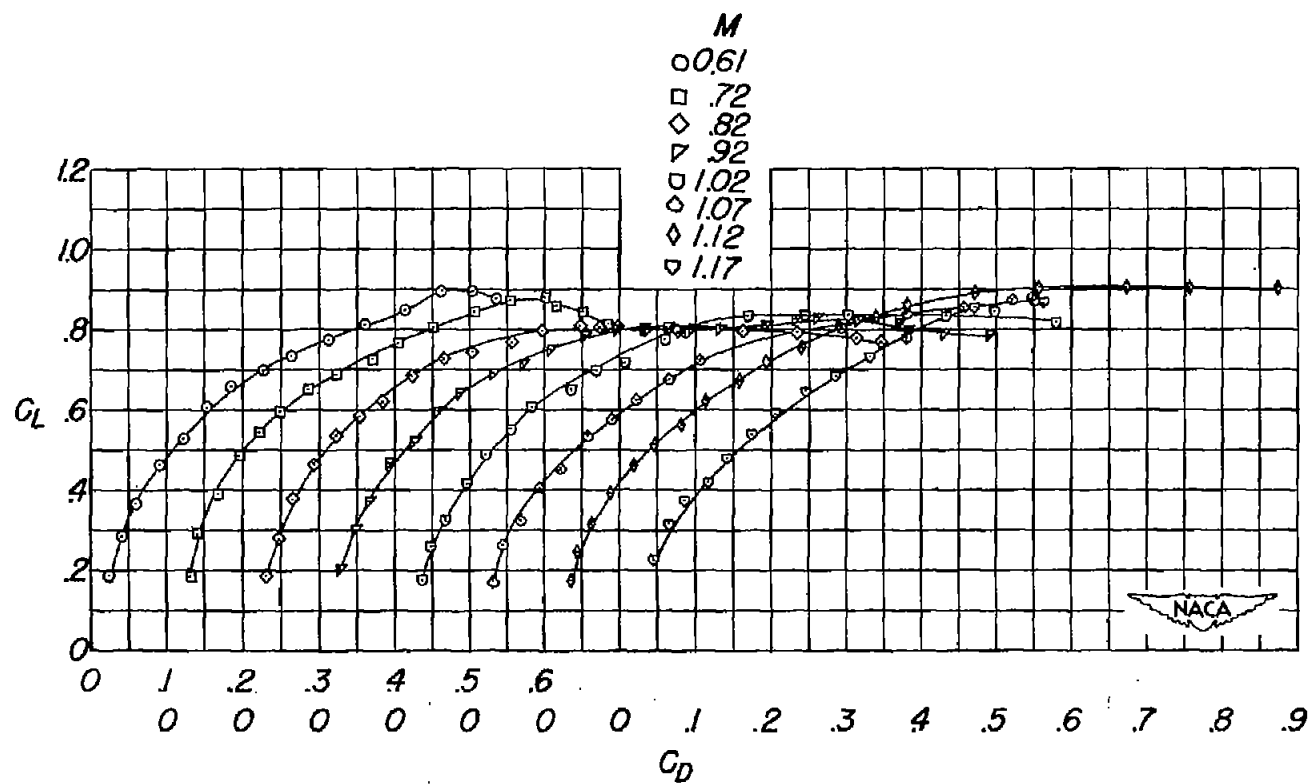


Figure 14.- Variation of drag coefficient with lift coefficient for an aspect-ratio-4 wing.  $\Lambda = 60^\circ$ .

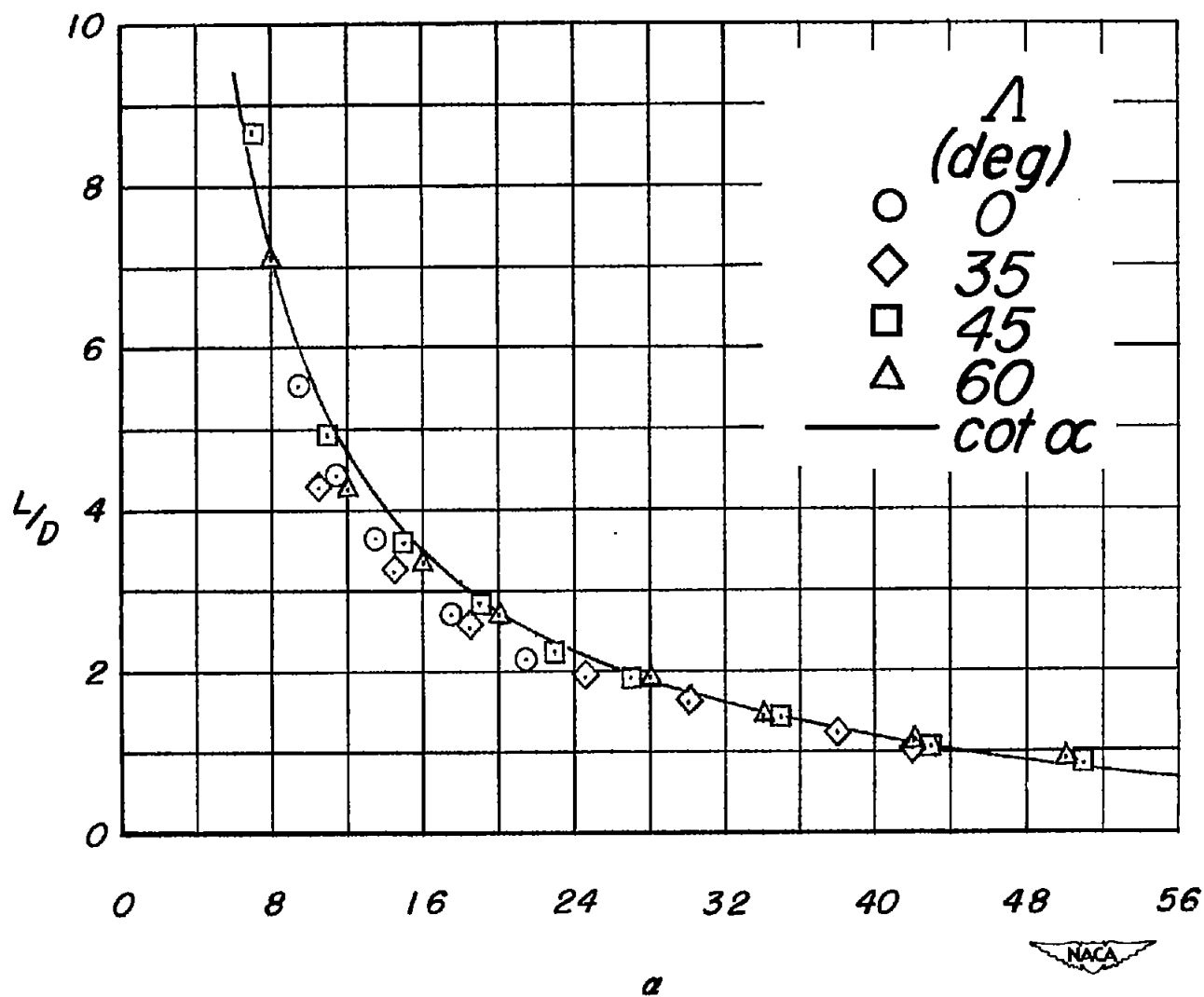


Figure 15.- Variation of lift-drag ratio with angle of attack for an aspect-ratio-4 wing.  $M = 0.92$ .

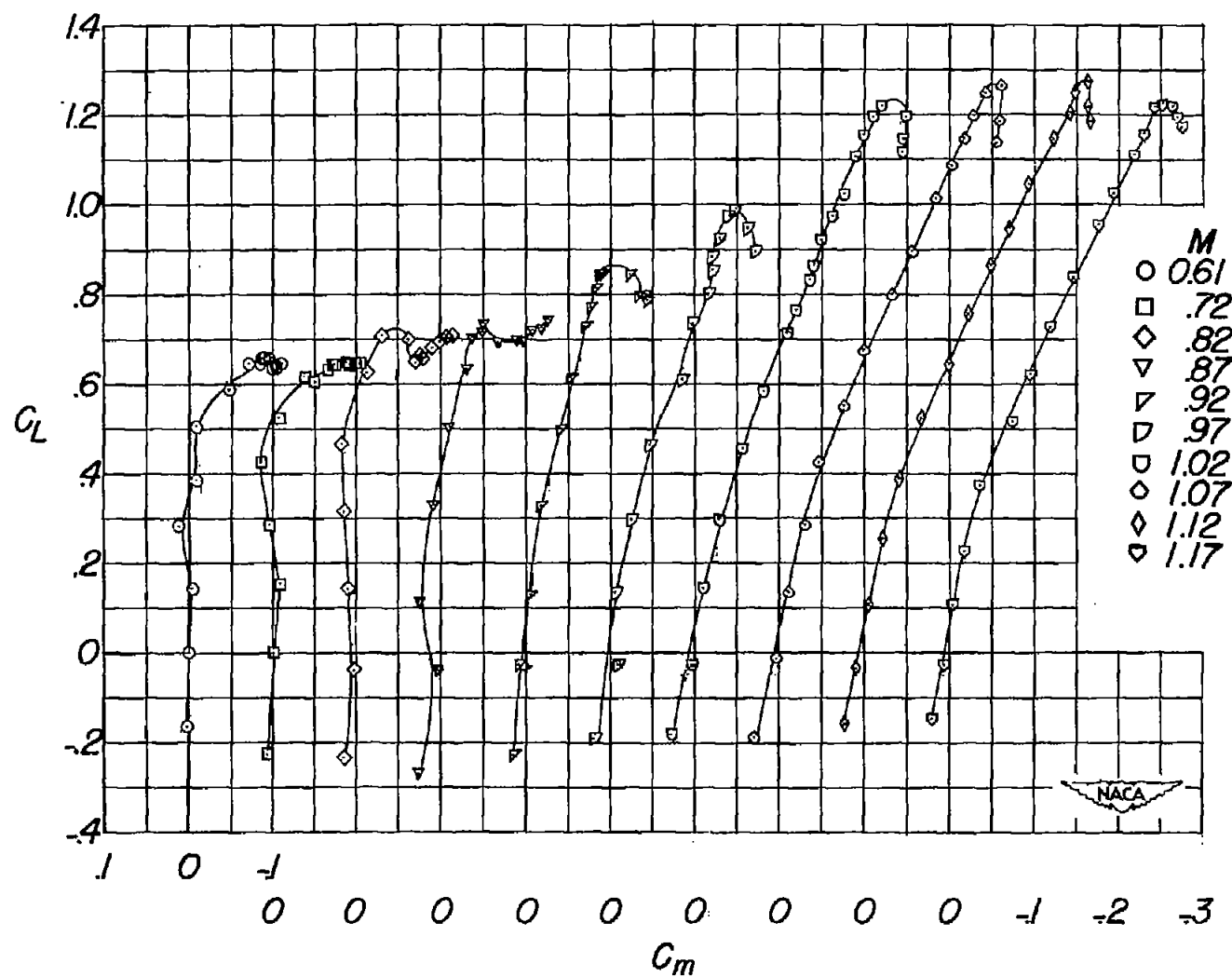


Figure 16.- Variation of pitching-moment coefficient with lift coefficient for an aspect-ratio-4 wing.  $\alpha = 0^\circ$ .

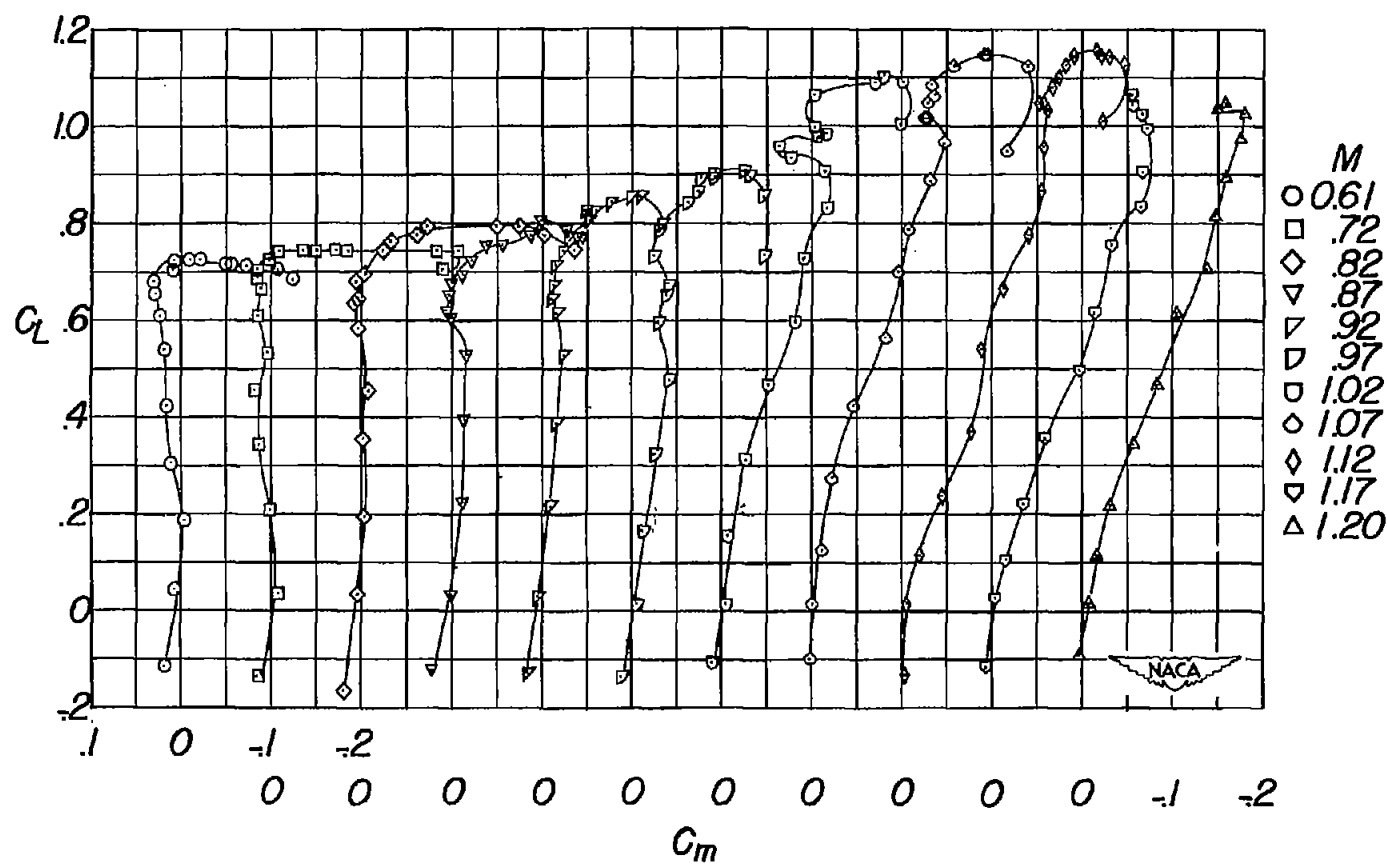


Figure 17.- Variation of pitching-moment coefficient with lift coefficient for an aspect-ratio-4 wing.  $\Lambda = 35^\circ$ .



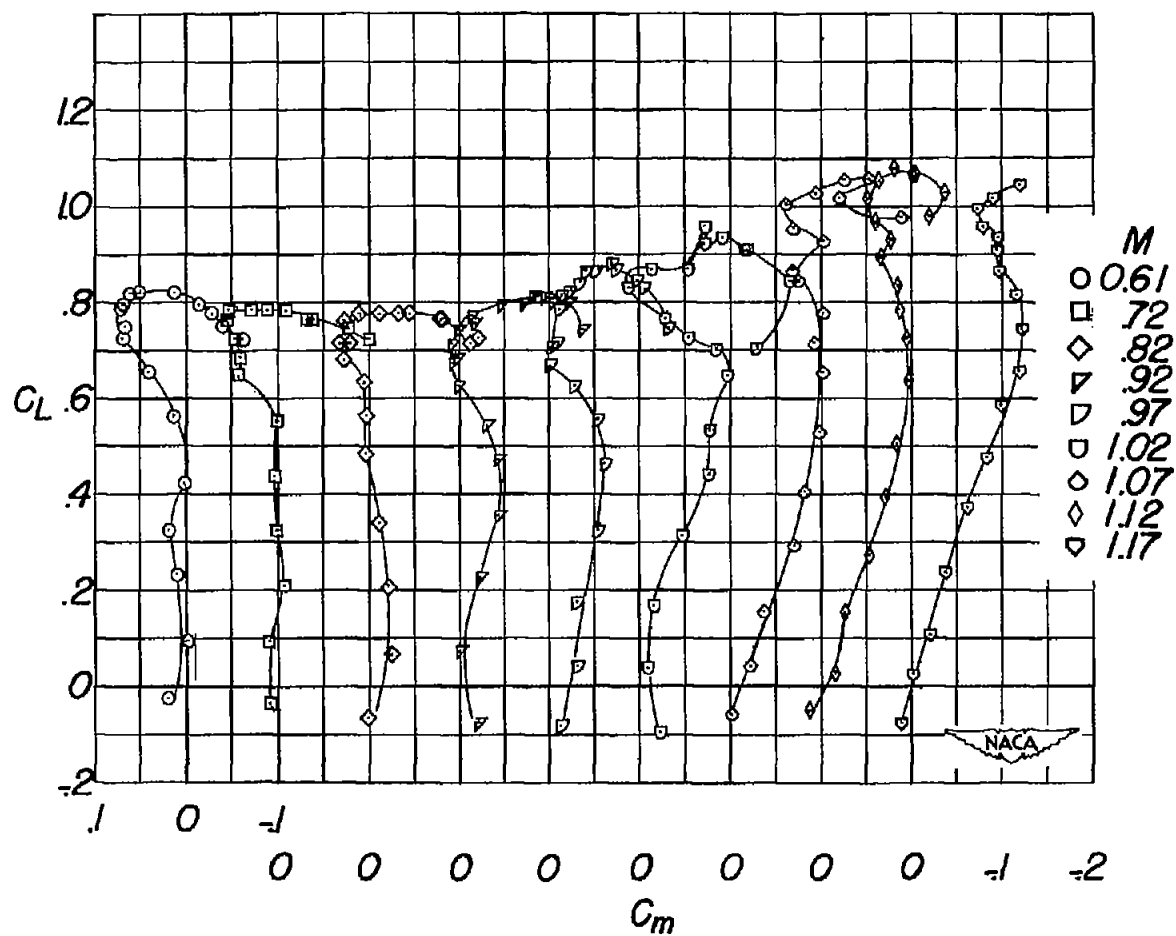


Figure 18.- Variation of pitching-moment coefficient with lift coefficient for an aspect-ratio-4 wing.  $\Lambda = 45^\circ$ .

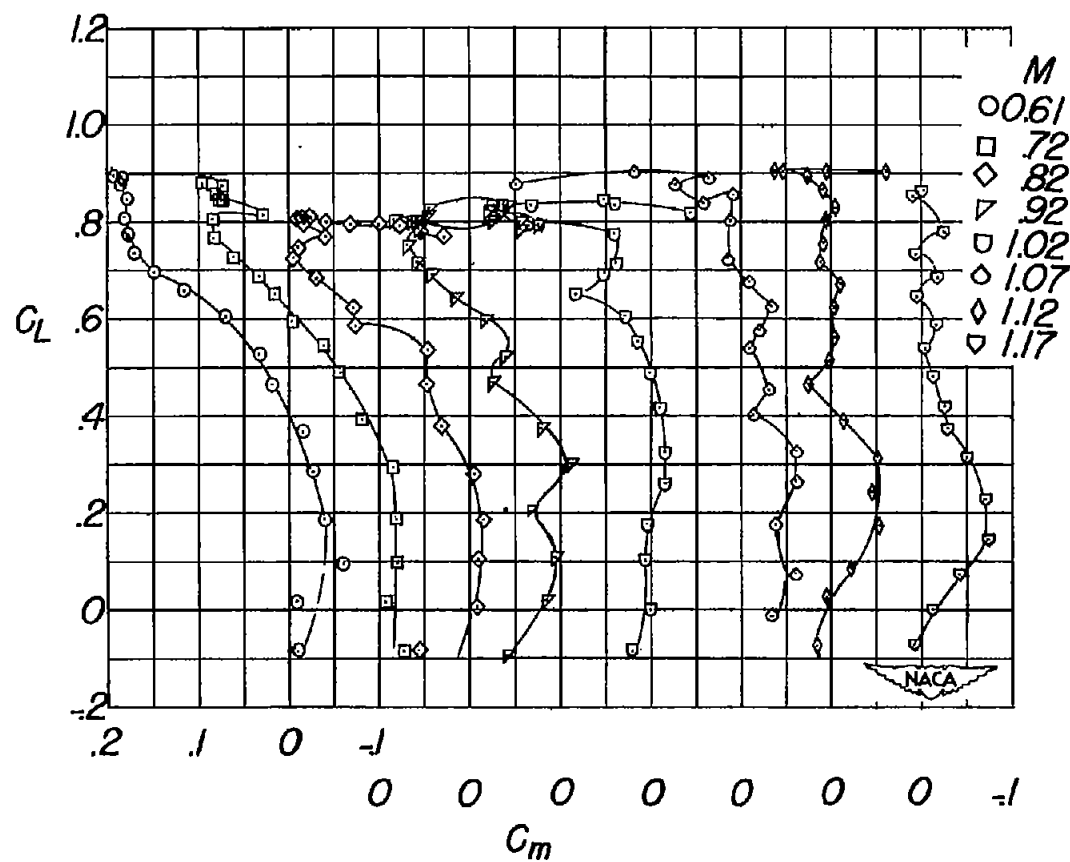


Figure 19.- Variation of pitching-moment coefficient with lift coefficient for an aspect-ratio-4 wing.  $\Lambda = 60^\circ$ .